DOI: 10.1002/chem.200801056

Crystallization Force—A Density Functional Theory Concept for Revealing Intermolecular Interactions and Molecular Packing in Organic Crystals

Tonglei Li,*[a] Paul W. Ayers,[b] Shubin Liu,[c] Matthew J. Swadley,[a] and Clare Aubrey-Medendorp[a]

Abstract: Organic molecules are prone to polymorphic formation in the solid state due to the rich diversity of functional groups that results in comparable intermolecular interactions, which can be greatly affected by the selection of solvent and other crystallization conditions. Intermolecular interactions are typically weak forces, such as van der Waals and stronger short-range ones including hydrogen bonding, that are believed to determine the packing of organic molecules during the crystal-growth process. A different packing of the same molecules leads to the formation of a new crystal structure. To disclose the underlying causes that drive the molecule to have various packing motifs in the solid state, an electronic concept or function within the framework of conceptual density functional theory has been developed, namely, crystallization force. The concept aims to describe the local change in electronic structure as a result of the self-assembly process of crystallization and may likely quantify the locality of intermolecular interactions that directs the molecular packing in a crystal. To assess the applicability of the concept, 5-methyl-2-[(2-nitrophenyl)amino]-3-thiophenecarbonitrile, so-called ROY, which is known to have the largest number of solved polymorphs, has been examined. Electronic calculations were conducted on the seven available crystal structures as well as on the single molecule. The electronic structures were analyzed and crystallization force values were obtained. The results indicate that the crystallization forces are able to reveal intermolecular interactions in the crystals, in particular, the close contacts that are formed between molecules. Strong correlations exist between the total crystallization force and lattice energy of a crystal structure, further suggesting the underlying connection between the crystallization force and molecular packing.

Keywords: density functional calculations · Fukui function · intermolecular interactions · polymorphism · solid-state structures

Introduction

Polymorphism, the ability of a solid material to exist in more than one form or crystal structure, is exceedingly important because of its relevance to structure–property relationships and the subtle and mysterious relationship between the structure and crystal packing of a molecule.[1] Polymorph control during crystallization is of practical significance because different forms possess different bulk properties, dissolution rates, chemical and physical stabilities, and bioavailabilities. The need for strict monitoring has led to polymorph screening during drug development to identify and characterize each form and to meet regulations. The search for all forms of a compound is typically achieved through an experimental screening process in which a compound is crystallized in various solvents or combinations of solvents under various conditions. It is virtually impossible, however, to know the number of likely polymorphs as well as their structures of a given organic molecule prior to a thorough screening being conducted. There exists no general understanding on the origin of the polymorphism of a compound or a general method to predict every possible polymorph.

Still, developing theoretical and computational tools for understanding polymorphism has been a continuous and

[a] Prof. Dr. T. Li, M. J. Swadley, C. Aubrey-Medendorp
Department of Pharmaceutical Sciences
University of Kentucky
Lexington, Kentucky (USA)
Fax: (+1) 859-257-7585
E-mail: tonglei@uky.edu

[b] Prof. Dr. P. W. Ayers
Department of Chemistry
McMaster University
Hamilton, Ontario (Canada)

[c] Dr. S. Liu
Renaissance Computing Institute
University of North Carolina
Chapel Hill, North Carolina (USA)

consistent effort. Current prediction methods generally rely on a brute-force approach to attempt to sort out all possible packing motifs of molecules in energy space to identify low-energy forms.[2] Because of the mammoth number of potential crystal-packing combinations and the lack of reliable and inexpensive energy models for evaluating molecular interactions, there has been limited success.[3] A recent effort, nevertheless, demonstrates a possibility of using a more vigorous energy evaluation method (similar to our method reported earlier[4]) to correctly predict polymorphs of a few relatively small organic molecules (under some specific assumptions of the crystal structures).[5]

To develop reliable methods for polymorph prediction, it is essential to understand the locality of intermolecular interactions and molecular moieties that determine the local interactions and consequent molecular-packing motifs in a crystal. Many studies have been carried out to analyze specific types of interactions in organic crystals, such as hydrogen bonding,[6] halogen bonding,[7] and π–π interactions.[8] Conversely, crystal engineering has sought to create unique crystal structures based on "synthons", or unique chemical moieties, that can "force" or direct molecules packed in particular patterns.[9] For example, various interaction motifs between different functional groups have been studied for producing organic cocrystals.[10] Nonetheless, current efforts are mostly of a qualitative, empirical nature, mainly relying on particular interactions such as hydrogen bonding, but falling short on generating insights on the subtle, rich diversity of organic chemical moieties forming intermolecular interactions that decide the polymorphism of an organic system.

To comprehend how intermolecular interactions influence the molecular packing and polymorphism of organic crystals, we have resorted to electronic calculations and analyses of the calculated electronic structures, particularly, by conceptual density functional theory (DFT). We have used Fukui functions for studying the origin of the polymorphic formation of a few organic systems including aspirin and indomethacin.[11] In this study, we present the results of the development and utilization of a new concept, "crystallization force", for quantifying the local interactions in one organic system that has the largest number of polymorphs solved by single-crystal X-ray diffraction analyses, namely, 5-methyl-2-[(2-nitrophenyl)amino]-3-thiophenecarbonitrile, or so-called ROY due to the red, orange, and yellow colors of its different forms.[12,13] ROY has been crystallized in at least ten polymorphs: yellow prisms (Y), yellow needles (YN), yellow plates (YT04), red prisms (R), orange needles (ON), orange plates (OP), and orange-red plates (ORP), whose structures have been solved and three others (R05, Y04, and RPL) whose structures have not been solved.[13] The molecule possesses three regions of torsional flexibility (Figure 1). Clearly, ROY offers a great challenge for understanding the polymorphism of organic crystals. Herein, we report the concept of crystallization force and its application to ROY.

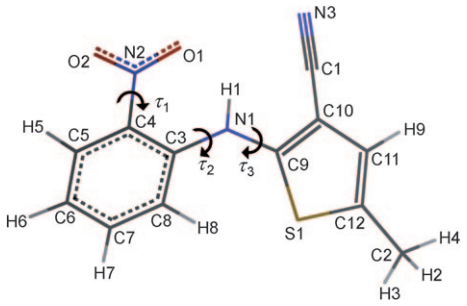

Figure 1. Molecular structure of ROY with atoms numbered. Three major dihedral angles are marked: τ_1 (O1-N2-C4-C3), τ_2 (C4-C3-N1-H1), and τ_3 (C3-N1-C9-C10).

Theory and Methods

In density functional theory (DFT), the electron density is the fundamental quantity for describing atomic and molecular ground states.[14] Accordingly, the total energy of a system (W) is dependent upon the energy of the electronic structure and of the nuclear–nuclear repulsion according to Equation (1), in which E is the electronic energy [defined in Eq. (2), in which $F[\rho]$ is the sum of the kinetic and electron–electron repulsion energy], V_{nn} is the nuclear–nuclear repulsion energy, $\rho(\mathbf{r})$ is the electron density at point $\mathbf{r}$ in space, and $v(\mathbf{r})$ is the external potential resulting from the positively charged nuclei.

$$W[\rho,v] = E[\rho,v] + V_{nn}[v] \tag{1}$$

$$E[\rho,v] = F[\rho] + \int \rho(\mathbf{r})v(\mathbf{r})d\mathbf{r} \tag{2}$$

From Equations (1) and (2), it is apparent that the energy of the system depends on both the electronic structure and nuclear–nuclear interactions. The energy fluctuation of a molecular system, or its chemical and/or structural stability, may be studied from perturbation–response perspectives on the mutual coupling between the electronic structure (electron density) and the molecular skeleton (nuclear charges and positions).[15] Redistribution of electrons may be regarded as a response to perturbations in the nuclear configuration. Conversely, one may regard changes in the electronic structure as perturbations leading to conformational changes. The relationship between responses and perturbations is the fundamental insight behind the DFT picture of chemical reactivity, which leads to novel conceptual tools for understanding chemical reactivity. These tools have been applied to complex molecular interactions and numerous chemical processes.[16,17] One important DFT concept for our study is the electronic Fukui function (EFF), $f(\mathbf{r})$, shown in Equation (3):

$$f(\mathbf{r}) = \left(\frac{\partial\rho(\mathbf{r})}{\partial N}\right)_v \tag{3}$$

in which N is the number of electrons. It is suggested that $f(\mathbf{r})$ is directly associated with the local polarizability or softness of a molecular system.[18] One approximate relationship (for atomic systems) is given by Equation (4):[19]

$$\alpha = S\int \mathbf{r}\mathbf{r}f(\mathbf{r})d\mathbf{r} \tag{4}$$

in which α and S are the global polarizability and softness, respectively. The softness, a DFT concept, can be dated back to Pearson's HSAB (hard and soft acids and bases) principle,[20,21] and may be utilized to characterize intermolecular interactions.[22,23] Among the three major contributions to the intermolecular interaction (i.e., electrostatic, covalent, and polarization) the hard–hard type of interaction is mainly electrostatic in nature, whereas the soft–soft type of interaction is of the covalent (sharing of electrons) and polarization characters.[21,24] For the or-

ganic crystals, the soft–soft type of intermolecular interaction is expected to be dominant. The local softness is defined as $Sf(\mathbf{r})$, so the Fukui function likely defines the spatial profile of a molecule's softness.[25] Consequently, a local region that has strong electronic Fukui functions is believed to contribute considerably to the local and overall intermolecular interaction, in particular, the van der Waals interaction, a major component of the lattice energy of organic crystals.[4] With regard to the molecular packing in the solid state, the van der Waals energies, together with the electrostatic interactions (which are less significant in molecular crystals), are believed to be relatively "flat" among the polymorphs of the same molecule. In other words, these long-range, nondirectional interactions form the baseline of the lattice energy of a polymorphic system and the small energy differences between polymorphs—as small as 2 kJ mol^{-1}, or even smaller—are mainly determined by interactions that are due to the favorable (electron sharing) or unfavorable (Pauli repulsion,[26] steric effect[27]) overlap of electron clouds, including close contacts, in which the interatomic distance is smaller than the sum of van der Waals radii, and hydrogen bonding. It is these short-range, directional intermolecular forces that are believed to be the determining factor for forming various packing motifs in organic crystals.

This covalent type of interaction, which is strongly directional, is also determined by the local softness. In fact, the Coulomb integral of Fukui functions (J_f) between two molecular systems, A and B, is shown to facilitate the electron sharing between the two molecules; the larger the J_f value, the more effective the electron transfer and sharing is expected to be.[22] As such, according to Equation (5), local regions with large Fukui functions can lead to strong intermolecular interactions—the closer these regions, the larger the interaction becomes—implying that the covalent type of interactions is highly directional and determined by the local chemistry of a molecule.

$$J_f = \int\int \frac{f(\mathbf{r})f(\mathbf{r}')}{|\mathbf{r}-\mathbf{r}'|}d\mathbf{r}d\mathbf{r}' \tag{5}$$

Although incipient covalent bonding may not be comparable to the overall van der Waals energy contribution by one molecule, it can be significant in a local region interacting with neighboring molecules. More importantly for this study, such a directional force, together with similar ones associated with other chemical moieties of the same molecule, is believed to regulate the molecular packing. This indicates that the Fukui function and local softness should be examined when seeking to understand the polymorphism of organic crystals.

In practice, since only the number of electrons, N, in a molecule can be changed by an integer, the EFF is resolved into nucleophilic ($f^{+}(\mathbf{r})$) and electrophilic ($f^{-}(\mathbf{r})$) components as shown in Equations (6a) and (6b), respectively:

$$f^{+}(\mathbf{r}) = \rho^{+}(\mathbf{r}) - \rho^{0}(\mathbf{r}) \tag{6a}$$

$$f^{-}(\mathbf{r}) = \rho^{0}(\mathbf{r}) - \rho^{-}(\mathbf{r}) \tag{6b}$$

Here $\rho^{+}(\mathbf{r})$, $\rho^{-}(\mathbf{r})$, and $\rho^{0}(\mathbf{r})$ are the electron densities of the anionic, cationic, and neutral molecular systems, respectively.[17,28] The EFF can be further extended to the nuclear Fukui function (NFF), $\mathbf{\Phi}_\alpha$, which is defined in Equation (7):[29]

$$\Phi_\alpha = \left(\frac{\partial \mathbf{F}_\alpha}{\partial N}\right)_\nu = Z_\alpha \int f(\mathbf{r})\frac{\mathbf{R}_\alpha - \mathbf{r}}{|\mathbf{R}_\alpha - \mathbf{r}|^3}d\mathbf{r} \tag{7}$$

in which $\mathbf{F}_\alpha$ is the Hellmann–Feynman force on nucleus α,[30] which has its nuclear charge of Z_α located at position $\mathbf{R}_\alpha$ in space. The connection between EFF and NFF shown by Equation (7) indicates that $\mathbf{\Phi}_\alpha$ can be used as a condensed representation of the EFF around nucleus α: a large NFF is typically associated with a large distribution of EFF. Similar to the EFF calculation, the NFF is also resolved into nucleophilic (Φ_α^+) and electrophilic (Φ_α^-) components as shown in Equations (8a) and (8b), respectively:[29]

$$\mathbf{\Phi}_\alpha^+ = \mathbf{F}_\alpha^+ - \mathbf{F}_\alpha^0 \tag{8a}$$

$$\mathbf{\Phi}_\alpha^- = \mathbf{F}_\alpha^0 - \mathbf{F}_\alpha^- \tag{8b}$$

in which $\mathbf{F}_\alpha^+$, $\mathbf{F}_\alpha^-$, and $\mathbf{F}_\alpha^0$ are the Hellmann–Feynman forces of the anionic, cationic, and neutral molecular systems, respectively.

The nuclear Fukui function is a local function that is associated with an individual nucleus and thus can be used to characterize local interactions. To understand crystal formation, however, the NFF needs to be normalized in accordance with the electronic perturbation associated with the vapor deposition process. (Crystallization from liquid to solid is beyond the scope of this report, but the same concept may be applicable for considering the solvent effect on crystal packing. For example, various polarizable continuum models may be used to calculate molecules in a solvent environment). In the crystallization process, the charges on the atoms in the molecule change by $dq_\alpha = q_\alpha(\text{gas}) - q_\alpha(\text{crystal})$. If dq_α is positive, then atom α accepts electrons during the crystallization process. The condensed EFF is defined in a way similar to that of the components in Equations (6a) and (6b), and represents the change in atomic charge (equivalently, the negative value of the change in atomic population) when electrons are added to or removed from a system [Eqs. (9a) and (9b)]:

$$f_\alpha^+ = q_\alpha^0 - q_\alpha^+ = n_\alpha^+ - n_\alpha^0 \tag{9a}$$

$$f_\alpha^- = q_\alpha^- - q_\alpha^0 = n_\alpha^0 - n_\alpha^- \tag{9b}$$

Here q_α^+, q_α^-, and q_α^0 and n_α^+, n_α^-, and n_α^0 denote the atomic charges and atomic populations on the anionic, cationic, and neutral molecular systems, respectively.[31,32] The quantity, dq_α/f_α^+ thus represents the number of electrons one would have to add to the molecule to change the charge on atom α by dq_α. That is, from the standpoint of atom α, crystallization "looks like" electron transfer of $dN_\alpha^{\text{eff}} = dq_\alpha/f_\alpha^+$ electrons. This effective electron transfer is associated with a force on the nucleus α as shown in Equation (10a). We refer to $\mathbf{G}_\alpha$ as the "crystallization force" on the atomic nucleus α. A similar analysis can be performed for atoms that lose electrons during the crystallization process, to yield Equation (10b):

$$\mathbf{G}_\alpha = \mathbf{\Phi}_\alpha^+ \frac{dq_\alpha}{f_\alpha^+} = \left(\frac{\partial \mathbf{F}_\alpha}{\partial N}\right)_\nu dN_\alpha^{\text{eff}} \quad \text{when } dq_\alpha > 0 \tag{10a}$$

$$\mathbf{G}_\alpha = \mathbf{\Phi}_\alpha^- \frac{dq_\alpha}{f_\alpha^-} \quad \text{when } dq_\alpha < 0 \tag{10b}$$

The crystallization force, $\mathbf{G}_\alpha$, can be regarded as the inherent NFF associated with crystallization. Due to its physical nature as a Hellmann–Feynman force, $\mathbf{G}_\alpha$ may thereby quantify the local binding force in a crystal. It should be noted that the definition given by Equations (10a) and (10b) assumes that there is no significant conformational change of a molecule from the gas to solid phase; only the changes in electronic structure are considered.

The "total crystallization force" (G) of a crystal is defined as the sum of magnitudes of individual crystallization forces [Eq. (11)]:

$$G = \sum_{\substack{\alpha \\ dq_\alpha > 0 \\ f_\alpha^+ > 0}} |\Phi_\alpha^+| \frac{dq_\alpha}{f_\alpha^+} - \sum_{\substack{\alpha \\ dq_\alpha < 0 \\ f_\alpha > 0}} |\Phi_\alpha^-| \frac{dq_\alpha}{f_\alpha^-} \tag{11}$$

It is expected that f_α^+ and f_α^- are positive. (It is possible that the condensed EFF can be negative for some atoms;[32–34] these atoms are excluded from the sum in Equation (11) because negative condensed EFFs are often associated with inadequacies in the population analysis method).[34] The total crystallization force, G, is expected to characterize the relative "ease" or binding force for molecules to form a crystal. It will be compared with the lattice energy as discussed later in the report.

To calculate Fukui functions and crystallization forces of ROY single crystals, the crystal structures were optimized with their lattice parameters held constant prior to the introduction of electronic perturbations

and calculations on the ionized electronic structures. The initial crystal structures were obtained from the Cambridge Structural Database with the reference codes of QAXMEH (ON), QAXMEH01 (Y), QAXMEH02 (R), QAXMEH03 (OP), QAXMEH04 (YN), and QAXMEH05 (ORP). The structure of the YT04 form was taken from the literature.[13] The electronic perturbations were initiated by adding or removing one electron from the unit cell of the optimized crystal structures for computing nucleophilic or electrophilic Fukui functions. The B3LYP exchange-correlation functional[35] and the 6-31G** basis set were selected for the DFT calculations. The structural optimizations and electronic calculations were conducted with a periodic quantum mechanical program, Crystal 03.[36] The program uses a background charge of the opposite sign to handle charged systems that were used to compute the Fukui functions. The energy convergence of the calculations was set to be 10^{-7} hartree. Root-mean-square (RMS) values were set to 0.0003 and 0.0012 atomic units (a.u.) for the energy gradient and atomic displacement, respectively. The same basis set and method were also used for calculating single ROY molecules to evaluate crystallization forces. The Mulliken population analysis was employed for obtaining the atomic charges for molecules in the crystal and gas phase. Electronic structures and properties calculated were visualized by using OpenDX.[37] A conformation-energy analysis of the single molecule was carried out regarding the three torsion angles (Figure 1) and, for this purpose, single ROY molecules were evaluated with B3LYP/6-311G** by using Gaussian 03.[38]

The lattice energy of the seven polymorphs of ROY was calculated with an empirically augmented density functional theory method that was tested on dozens of organic crystals.[4,39] The method was shown to be satisfactory in comparison to experimental values. The original method had parameters that could only handle C, N, O, and H atoms. The atomic dispersion coefficient and effective number of electrons of S were taken from the Halgren's report as 1383.84 kcal mol^{-1} Å^3 and 4.8, respectively.[40] The van der Waals radius of S was assigned as 1.80 Å according to the literature.[41] The optimized crystal structure of the seven polymorphs of ROY was used in both the empirical and DFT calculations of the lattice energy.

Results and Discussion

To understand the intermolecular interaction and its role in the molecular packing of ROY, conformations of a single molecule were analyzed and are presented first in this section, followed by results of Fukui functions. Crystallization forces are then discussed, along with their correlation to the lattice energies of the seven polymorphs.

Conformational analysis: Upon analysis of the conformation of ROY molecules in each polymorph, it is found that three particular dihedral (torsion) angles have distinct values (Table 1). The flexibility of these dihedral angles, denoted τ_1–τ_3 in Figure 1, is the aspect of the molecular structure of ROY that is responsible for the its structural diversity; different choices for the dihedral angles lead to very different crystal packing motifs. τ_1 represents the rotation of the nitro group relative to the phenyl ring, whereas τ_2 and τ_3 represent the planes of the nitrophenyl and five-membered ring, respectively. From an electronic structure standpoint, ROY would prefer to be a planar molecule, with a delocalized aromatic system spanning both the phenyl and thiophene rings and their connecting amino group, as well as the nitro group. Steric factors prevent this from occurring, with the extent of nonplanarity clearly illustrated by the nonzero τ_1–τ_3 values in the molecules of every polymorph, as well as the optimized ROY single molecule. The comparative values of τ_1 and τ_2 determine the length of the intramolecular hydrogen bond that forms between O1 and H1 in the structure, which has a length variance between about 1.9 and 2.1 Å in each polymorph. In theory, O1 and H1 would be expected to lie in the same plane as the phenyl ring to both delocalize the aromatic system and minimize the length of the hydrogen bond formed between them. However, the skewing illustrated by the molecular structure of each polymorph (along with the optimized molecular structures) suggests otherwise.

Table 1. Values of dihedral angles (τ in degrees) of interest in each ROY polymorph as well as the optimized single molecule in the gas phase.

	ON	OP	ORP	R	Y	YN	YT04	Molecule
τ_1	4.45	−18.73	−3.55	−18.30	1.74	−3.58	14.65	−6.29
τ_2	−5.83	14.56	1.37	10.09	11.80	−11.93	−10.31	7.72
τ_3	−44.68	35.99	35.55	34.46	−121.11	122.60	112.58	−121.79

To understand how the conformational diversity of the ROY single molecule may influence the polymorphism, conformational analyses of the single molecule were carried out. Conformers were generated by altering the dihedral angles of the optimized single molecule in the spans of $\tau_1 = -20$ to $+20°$, $\tau_2 = -120$ to $+120°$, and $\tau_3 = -180$ to $+180°$ with a 5° increment by modifying the optimized geometry, and their energies were calculated. Figure 2 shows

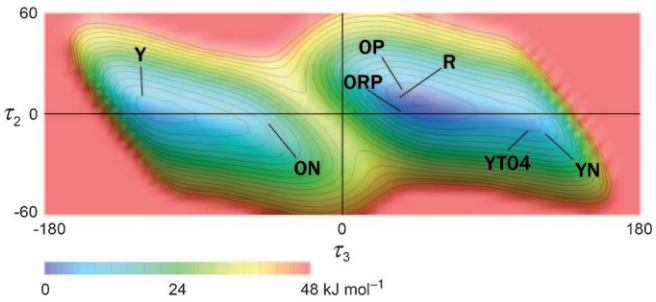

Figure 2. Energy space of a single ROY molecule as a function of τ_2 and τ_3 with corresponding values of molecules in the polymorphs marked. τ_1 was as kept as zero. The color spectrum bar indicates the relative energy scale; each contour line represents an energy change of 3 kJ mol^{-1}.

the energy map of τ_2 versus τ_3 with $\tau_1 = 0°$. Corresponding ROY polymorphs are overlaid upon the energy map in accordance with their τ_2 and τ_3 values. It can be seen that two major energy minima occur at approximately ($\tau_3 = -120$, $\tau_2 = 5°$) and ($\tau_3 = 40$, $\tau_2 = 10°$). The values of τ_1–τ_3 have symmetry implications for the ROY single molecule (Figure 1). The mirror image of a molecule can be obtained by multiplying the values of these three dihedral angle values by −1, indicating that there should be an axis of symmetry at the line $\tau_2 = \tau_3$ (since $\tau_1 = 0$). The lack of symmetry in Figure 2 is primarily because τ_1 was fixed to be zero, but the fact that the energies of the conformers were calculated without structural optimization may also be a factor. Similar plots of

τ_2 versus τ_3 with slight shifts of the energy map were obtained (results are not shown) when τ_1 was given different values within $\pm 20°$.

To establish the existence of the mirror images of the found local minima, full optimizations were performed for a ROY single molecule (Table 2). By starting the optimizations at differing τ_3 values, four energy local minima of the ROY molecule were identified. The results verified the existence of symmetric energy minima in mirror-image conformations. Those started at $\tau_3 = -120$ and $+120°$ had the same energy and effectively opposite τ values. The same was true for those started at $\tau_3 = -50$ and $+50°$. Clearly, the energy space of a ROY single molecule should be symmetric with four local minima (Table 2). The nonzero τ_1 and τ_2 values of the optimal single molecular structures further suggest that the molecule cannot form the delocalized, aromatic system among the phenyl, thiophene, nitro, and amino groups.

Table 2. Dihedral angles (in degrees) and relative energies (in kJ mol^{-1}) of a single ROY molecule optimized in the gas phase with different initial τ_3 values.

	Initial τ_3 value			
	−120.00	−50.00	50.00	120.00
final τ_1	−6.29	8.76	−8.74	6.23
final τ_2	7.72	−10.77	10.73	−7.65
final τ_3	−121.79	−42.01	42.13	121.71
relative energy	0.00	+0.10	+0.10	0.00

As illustrated in Figure 2, all of the ROY polymorph conformations tend to align with the local minima of the single molecule with regard to τ_2 and τ_3. The τ_1 values of the polymorphs are also within the range of those of optimized single molecules. The difference in any of τ_1–τ_3 values between the polymorphs (Table 1) and local minima (Table 2) is less than 10°. Clearly, the four local energy minima of the ROY molecule are not the sole source of the large number of polymorphs of the compound. The existence of a few polymorphs within the vicinity of one local minimum has to be related to intermolecular interactions and molecular packing in the solid state. Moreover, intermolecular hydrogen bonding appears to play a minor role in the intermolecular interactions of the polymorphs of ROY. The molecular structure of ROY (Figure 1) has two hydrogen-bonding acceptors ($-NO_2$ and $-CN$), but lacks a donor, except for the amino group, that is likely to form intramolecular hydrogen bonding with the nitro group. On the contrary, several close contacts are identified in each polymorph. A close contact between two atoms is indicated by the interatomic distance that is smaller than the sum of their van der Waals radii, which suggests overlap of their electron clouds. The existence of close contacts in the crystals is expected to contribute considerably to the intermolecular interactions, in particular, the short-range forces that are of covalent character and due to the sharing of electrons. The diversity of the close contacts is perhaps the main factor that controls the polymorphism of the compound in addition to the conformational flexibility discussed above.

Fukui functions: Electronic and nuclear Fukui functions were calculated for each of the ROY polymorphs. The functions are believed to describe intrinsic attributes of a crystal structure, most likely, the local polarizability and intermolecular interactions that stem from electron sharing (e.g., hydrogen bonding and close contact). Illustrated in Figures 3 and 4 are the Fukui functions calculated for the ON and other six polymorphs, respectively. In Figure 3a, it is clear that the -NO_2 group in the ON form has the largest distribution of nucleophilic EFF, followed by the C7, C3, and N1. Conversely, the electrophilic EFFs (Figure 3b) have large distributions around the amino group, part of the five-membered ring (C10–C12), N3, and C6 and C8 of the phenyl group. Magnitudes of the NFFs, indicated by arrows in the figure (values in Table 3), seem to correspond well with the

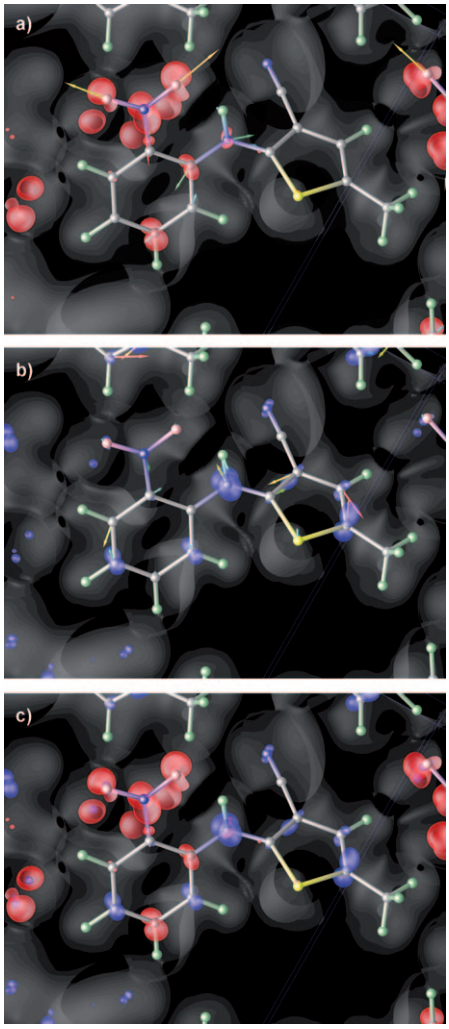

Figure 3. Isosurfaces of EFFs (0.002 a.u.) of ON superimposed with isosurfaces of electron density (0.01 a.u.) in gray: a) the nucleophilic in red, b) the electrophilic in blue, and c) both. Corresponding NFFs are also illustrated as arrows in (a) and (b), respectively. Arrow lengths increase with increasing relative magnitudes, and their colors also change from blue to green to red. Note that not all molecular structures are shown in the view.

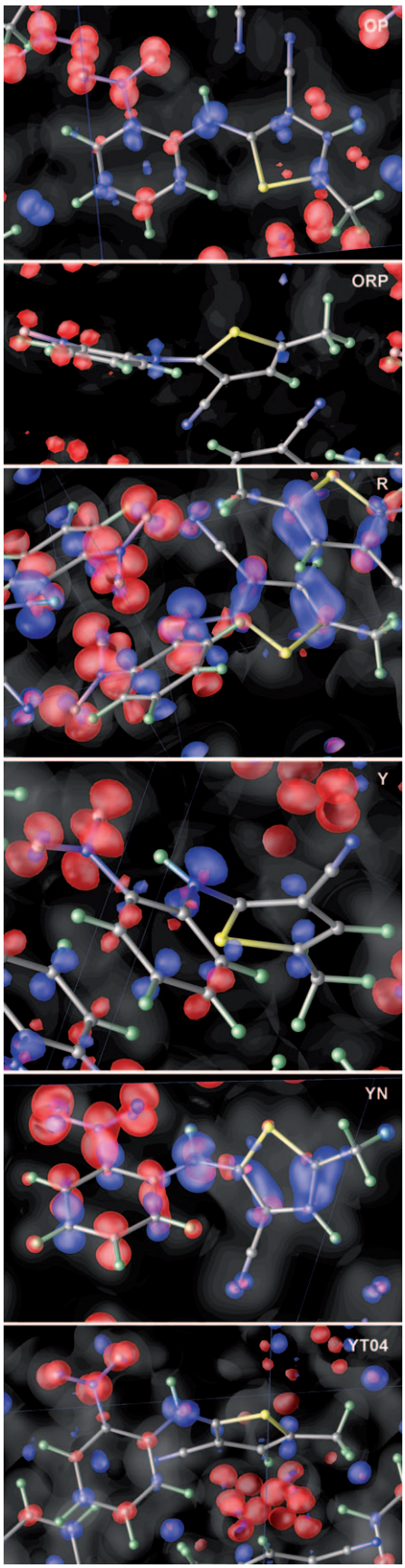

Figure 4. Isosurfaces of EFFs (0.002 a.u.) of all polymorphs but ON superimposed with isosurfaces of electron density (0.01 a.u.) in gray. Nucleophilic EFFs are in red and electrophilic in blue. Note that not all molecular structures are shown in the view.

EFFs, with the nitro group (mainly N2) holding the largest values. Figure 4 shows distributions of EFFs of other polymorphs. For example, the nitro group in the YN form has the largest distribution of nucleophilic EFF as well as the largest corresponding nucleophilic NFFs (Table 3). Its whole phenyl ring and the amino groups also have large distributions of EFFs. The five-membered ring and the amino group bear significant distributions of electrophilic EFFs; so does the aromatic ring. The NFFs are commensurate with the electronic counterparts. Fukui functions in other polymorphs demonstrate similar yet distinct distributions. The nitro groups have the largest distributions of nucleophilic EFFs. Because a large NFF value generally characterizes a large distribution of EFFs around the nucleus, correspondingly, O1, O2, and N2 of the nitro group in each polymorph have the largest nucleophilic NFFs (Φ_α^+), as listed in Table 3. The next largest NFFs are found on the carbon atoms of the aromatic ring. H1, in general, has smaller NFFs than non-hydrogen nuclei, but its values are outstanding among any other hydrogen nuclei of ROY: $|\Phi_\alpha^+|$ on H1 are 3 to 4 times larger than the next largest hydrogen atom. Conversely, it is the other half of the molecule that has the largest electrophilic NFFs (Φ_α^-), including the N1 and the four carbon atoms of the five-membered ring (C9–C12). H1 of the amino group again exhibits the largest values among hydrogen atoms. The results of all of the polymorphs show that the NFFs closely match the EFFs and the largest $|\Phi_\alpha^+|$ values for each structure are about 2 times more than the largest $|\Phi_\alpha^-|$ values. The larger values of $|\Phi_\alpha^+|$ may stem from the electron distribution in an anion extending to outer, less spherically symmetric orbitals; by contrast, the occupied orbitals in the cation are expected to be more similar to those from the neutral molecule.

Crystallization forces: The Fukui functions discussed earlier represent inherent properties of a crystal structure. They are evaluated upon electronic perturbation of a crystal and are thereby determined by the change in the electronic structure of the crystal that is caused by the perturbation [i.e., ∂N in Eq. (3)]. The perturbation is "artificially" introduced for the calculation by varying the number of electrons in the system. It has little physical connection but acts as a mathematic procedure for obtaining Fukui functions. Because of the relationship between the Fukui function and electronic perturbation, values of Fukui functions are influenced by the way and extent in which the perturbation is introduced: the larger the perturbation, the larger the distribution of Fukui functions. The values can also be affected by the number of molecules in a unit cell and the size of the unit cell, making it difficult to compare Fukui functions among different polymorphs.

In contrast, crystallization force, $\mathbf{G}_\alpha$, defined in Equations (10a) and (10b), considers the electronic perturbation pertinent to the crystallization process. It is evaluated as a normalized NFF based on the ratio of the change in atomic charge from the gas to the crystalline phase, dq_α, and the change originating from the electronic perturbation for cal-

Table 3. Magnitudes of nucleophilic NFFs (Φ_α^+ in nN) and electrophilic NFFs (Φ_α^- in nN) of each ROY polymorph.

	ON		OP		ORP		R		Y		YN		YT04	
	$\lvert\Phi_\alpha^+\rvert$	$\lvert\Phi_\alpha^-\rvert$	$\lvert\Phi_\alpha^+\rvert$	$\lvert\Phi_\alpha^-\rvert$	$\lvert\Phi_\alpha^+\rvert$	$\lvert\Phi_\alpha^-\rvert$	$\lvert\Phi_\alpha^+\rvert$	$\lvert\Phi_\alpha^-\rvert$	$\lvert\Phi_\alpha^+\rvert$	$\lvert\Phi_\alpha^-\rvert$	$\lvert\Phi_\alpha^+\rvert$	$\lvert\Phi_\alpha^-\rvert$	$\lvert\Phi_\alpha^+\rvert$	$\lvert\Phi_\alpha^-\rvert$
S1	0.128	0.206	0.107	0.223	0.056	0.114	0.301	0.426	0.051	0.202	0.213	0.524	0.023	0.233
O1	1.442	0.101	1.307	0.108	0.632	0.048	2.155	0.162	1.408	0.101	2.382	0.173	1.376	0.109
O2	1.213	0.130	1.247	0.136	0.664	0.059	2.521	0.213	1.295	0.151	2.681	0.354	1.249	0.150
N1	0.706	0.473	0.523	0.452	0.387	0.337	1.195	1.058	0.512	0.401	1.150	0.768	0.548	0.404
N2	1.608	0.333	1.413	0.338	0.811	0.137	2.903	0.594	1.697	0.353	3.344	0.757	1.583	0.350
N3	0.023	0.011	0.039	0.023	0.043	0.021	0.232	0.092	0.060	0.027	0.095	0.024	0.041	0.012
C1	0.076	0.080	0.141	0.097	0.076	0.061	0.479	0.250	0.071	0.106	0.191	0.187	0.057	0.090
C2	0.020	0.099	0.017	0.156	0.010	0.075	0.127	0.218	0.021	0.113	0.032	0.344	0.016	0.113
C3	0.768	0.201	0.498	0.165	0.383	0.135	1.047	0.100	0.633	0.238	1.474	0.391	0.640	0.239
C4	0.644	0.235	0.639	0.214	0.382	0.072	1.632	0.389	0.891	0.265	1.689	0.546	0.698	0.312
C5	0.040	0.470	0.140	0.415	0.091	0.140	0.581	0.579	0.252	0.426	0.477	0.766	0.129	0.555
C6	0.246	0.274	0.091	0.214	0.083	0.087	0.328	0.296	0.124	0.203	0.258	0.415	0.125	0.322
C7	0.387	0.103	0.258	0.102	0.214	0.042	0.543	0.132	0.394	0.117	0.929	0.175	0.352	0.113
C8	0.416	0.148	0.237	0.144	0.221	0.049	0.488	0.234	0.426	0.178	1.019	0.230	0.364	0.176
C9	0.551	0.425	0.342	0.408	0.310	0.372	1.250	1.077	0.287	0.189	0.751	0.696	0.300	0.305
C10	0.057	0.530	0.177	0.484	0.084	0.339	0.549	1.245	0.048	0.392	0.238	1.100	0.090	0.419
C11	0.089	0.669	0.039	0.645	0.045	0.409	0.160	1.499	0.053	0.491	0.089	1.159	0.053	0.573
C12	0.124	0.592	0.054	0.547	0.068	0.339	0.198	1.247	0.051	0.383	0.087	0.866	0.052	0.436
H1	0.199	0.276	0.167	0.243	0.127	0.121	0.462	0.520	0.139	0.22	0.370	0.398	0.170	0.272
H2	0.039	0.024	0.030	0.033	0.024	0.022	0.013	0.078	0.021	0.023	0.087	0.088	0.017	0.019
H3	0.017	0.044	0.066	0.068	0.018	0.025	0.051	0.066	0.032	0.056	0.084	0.066	0.024	0.056
H4	0.043	0.029	0.008	0.022	0.022	0.008	0.180	0.043	0.028	0.029	0.139	0.108	0.030	0.023
H5	0.015	0.018	0.055	0.018	0.041	0.006	0.125	0.030	0.061	0.021	0.120	0.034	0.066	0.023
H6	0.052	0.015	0.006	0.033	0.033	0.009	0.124	0.046	0.011	0.024	0.041	0.044	0.017	0.030
H7	0.043	0.015	0.019	0.009	0.031	0.003	0.116	0.015	0.032	0.012	0.062	0.008	0.006	0.017
H8	0.025	0.032	0.040	0.037	0.005	0.012	0.020	0.050	0.023	0.031	0.042	0.057	0.085	0.035
H9	0.093	0.031	0.021	0.017	0.013	0.016	0.025	0.071	0.097	0.037	0.019	0.055	0.070	0.046

culating the NFF, f_α. As such, $\mathbf{G}_\alpha$ is believed to characterize the intrinsic intermolecular interaction defined by the self-assembly process. In addition, because of the normalization process, $\mathbf{G}_\alpha$ can be compared numerically among different polymorphs with respect to the local intermolecular interaction.

Crystallization forces of the seven polymorphs were calculated and are listed in Table 4. They are also illustrated in Figure 5. In the ON form, the largest value is on C4 (1.6104 nN). However, its f_α value is smaller than zero, meaning that the atom actually loses electrons in the anionic form when calculating the nucleophilic Fukui functions. Because the decrease was very small (about 0.1 % of an electron as compared with the average change of 1.2 % for all non-hydrogen atoms), the negative value and subsequent $\mathbf{G}_\alpha$ may be an artifact caused by the calculation and population analysis methods. For similar reasons, the f_α value of H9 is also negative. Therefore, in this study, for those nuclei whose f_α were negative, their crystallization forces were excluded from the illustration in Figure 5 as well as in calculating the total crystallization force of a crystal system. With C4 ignored in the ON form, $\mathbf{G}_\alpha$ of N2 of the nitro group becomes the largest value, followed by that of the N1 of the amino with its H1 bearing the largest value among all hydrogen atoms. Crystallization force values of both C8 and C6 of the phenyl ring and the two atoms, C1 and N3, of the nitrile group are significant as well. C11 of the thiophene also has a considerable crystallization force value. Because $\mathbf{G}_\alpha$ is evaluated based on either Φ_α^+ or Φ_α^- depending on the sign of dq_α [Eq. (10)], large values of some NFFs may not be necessarily carried over into $\mathbf{G}_\alpha$. The $\mathbf{G}_\alpha$ of O1 and O2 of the nitro group are calculated based on Φ_α^- due to their dq_α

Table 4. Crystallization forces (in nN) and the total crystallization forces (G in nN).

	ON	OP	ORP	R	Y	YN	YT04
S1	0.0025	0.1043	0.1951	0.1350	0.0738	0.0590	0.0022
O1	0.1736	0.0026	0.4347	0.3102	0.4360	0.0679	0.0038
O2	0.1685	0.4804	0.1342	0.2151	0.1986	0.0712	0.1048
N1	1.2003	1.0137	1.0916	1.8555	1.5761	0.8128	1.2799
N2	1.5136	1.9156	1.8523	1.0227	1.0086	2.1914	0.0174
N3	0.4259	0.4612	4.8867	1.0530	1.9501	0.5813	0.6778
C1	0.6277	0.7202	0.9436	0.9141	1.5967	0.9046	0.0141
C2	0.0979	0.1119	0.1866	0.4171	0.2457	0.1098	0.0748
C3	0.0477	0.0120	0.0411	0.0663	0.3343	0.1459	0.1239
C4	1.6104[a]	0.0920	0.0358	0.1049	0.2798	0.1918	0.0021
C5	0.1235	0.0384	0.1653	0.1572	0.1795	0.1365	0.0660
C6	0.4802	0.2327	1.6244[a]	0.7737	0.7408	1.0485	0.3625
C7	0.1907	0.0835	0.6770	0.2513	0.7631	0.9526	0.2197
C8	1.1125	0.3992	0.3062	0.9144	0.5039	1.1403	0.7456
C9	0.0486	0.0572	0.0492	0.2563	0.0869	0.1009	0.5402
C10	0.0478	0.6152	0.4810	0.1223	0.0784	0.0192	0.1043
C11	0.3408	0.2120	0.3977	0.3062	0.8428	0.0471	0.0800
C12	0.0259	0.0320	0.0234	0.0008	0.1384	0.0489	0.0029
H1	0.1806	0.0980	0.2660	3.9523	0.9982	0.0971	0.0064
H2	0.1038	0.0826	0.0204	0.0502	0.0772	0.1340	0.1815[a]
H3	0.0132	0.1051	0.2223	0.0078	0.2131	0.1287	0.0022
H4	0.1030	0.0079	0.0868	0.0609	0.0770	0.0430	0.2476
H5	0.0563	0.0838	0.0891	0.0399	0.0216	0.0220	0.0005
H6	0.0243	0.1590	0.0569	0.0597	0.0251	0.0522	0.0014
H7	0.0756	0.0152	0.0277	0.0249	0.0487	0.0188	0.0002
H8	0.0240	0.0397	0.0930	0.0964	0.0320	0.0836	0.0006
H9	0.0910[a]	0.0251	0.1267	0.1431	0.1299	0.0534	0.0651[a]
G	7.2084	7.2006	12.8904	13.3112	12.6556	9.1606	4.6811

[a] $f_a^+ < 0$.

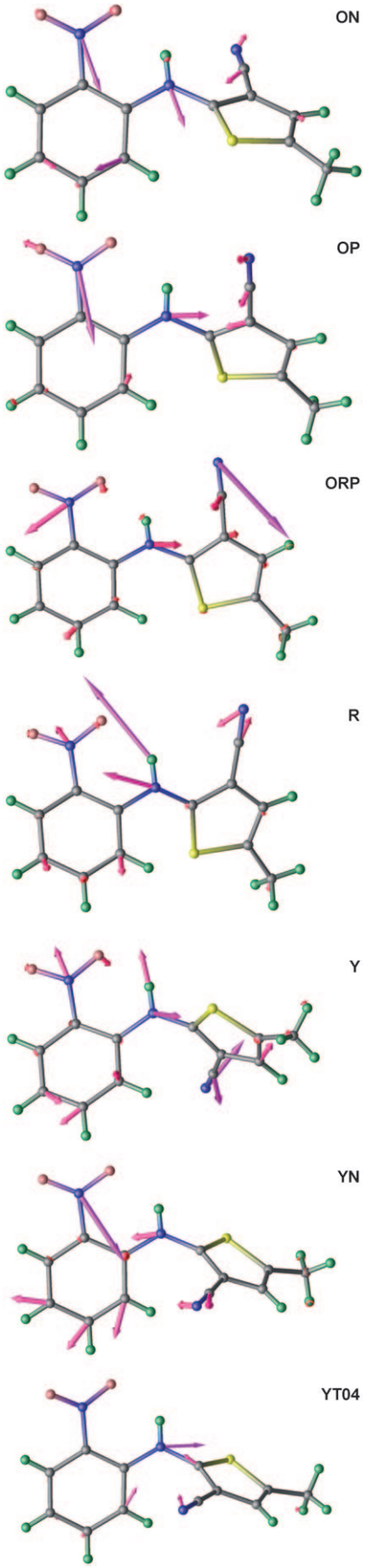

Figure 5. Crystallization forces of the seven polymorphs illustrated by pink arrows indicating both directions and relative magnitudes.

being negative (meaning both atoms do not gain more electrons on moving from the gas to solid phase), which results in small values. In the ON form, three close contacts are identified that include O1···H9 and O2···H9 of 2.67 Å and N3···H7 of 2.59 Å. Although $\mathbf{G}_\alpha$ values of O1 and O2 are insignificant, the largest value of N2 suggests that the nitro group, which is a π-conjugated system and shares their valence electrons, may indeed interact strongly with neighboring molecules forming the close contacts with H9. In addition, C11 that hosts H9 also shows a significant $\mathbf{G}_\alpha$. The third close contact of N3···H7 is synonymic with the large values of $\mathbf{G}_\alpha$ of the nitrile group. The amino group has no close contact or hydrogen bonding with other molecules, but it forms the intramolecular hydrogen bond with the flanking nitro group in both gas and solid phases. As such, the large $\mathbf{G}_\alpha$ of N1 may epitomize the impact of intermolecular interactions, particularly those associated with the nitro group, which is the hydrogen-bond acceptor (i.e., the O1/O2···H9 close contacts), on the intramolecular hydrogen bond. Moreover, phenyl rings stack upon each other in the crystal with a distance between corresponding atoms of 3.94 Å, likely resulting in the large $\mathbf{G}_\alpha$ of C8 and C6.

Similar results of crystallization forces are found in other polymorphs. Large values of $\mathbf{G}_\alpha$, in general, signify close contacts between molecules in the crystal structures. In the OP form, N2 of the nitro group has the largest $\mathbf{G}_\alpha$, although that of the terminal O2 is also significant. Two close contacts, O2···O2 (3.00 Å) and O2···H2 (2.68 Å), are found originating from the nitro group. The two atoms of the nitrile group (N3 and C1), together with the anchor atom, C10, have large $\mathbf{G}_\alpha$ values, and subsequently lead to an intermolecular hydrogen bond, H1···N3 (2.62 Å), and another close contact, H6···N3 (2.68 Å). In addition to the intermolecular hydrogen bond, the amino group forms an intramolecular hydrogen bond with the nitro group, causing a large $\mathbf{G}_\alpha$ for N1. The last close contact identified is between two hydrogen atoms, H6···H4 (2.30 Å); interestingly, H6 shows a significant $\mathbf{G}_\alpha$ relative to other hydrogen atoms. Moreover, phenyl rings are stacked alternatively with the thiophene groups with an interplane distance of about 4 Å, producing significant $\mathbf{G}_\alpha$ on C6, C8, C10, and C11. In the ORP form, N3 has a significantly large value of $\mathbf{G}_\alpha$ (4.8867 nN), the largest one found among all atoms in the seven polymorphs, and is involved in one of three close contacts (N3···H9, 2.59 Å). The other two close contacts are with the nitro group (O2···H2, 2.70 Å; O1···H7, 2.50 Å), which has a large $\mathbf{G}_\alpha$ on O1 and N2. The amino group has a significant $\mathbf{G}_\alpha$ as well. Stacking of phenyl rings in the crystal shows an interplane distance of more than 6 Å, whereas thiophene rings are piled more compactly (about 4 Å). In the R form, the largest $\mathbf{G}_\alpha$ values are seen on the amino group with H1 having a surprisingly large value (3.9523 nN). Although the group does not participate in any close contact or intermolecular hydrogen bonding, the large values may stem from its intramolecular hydrogen bond with the nitro group, which produce four of six close contacts identified in the crystal structure (O1···H7, 2.70; O1···O1, 2.97; O1···N2, 3.03;

O2···H2, 2.50 Å). The intramolecular hydrogen bond appears to experience a significant impact when the molecule "moves" from the gas to solid phase. The other two close contacts are found with the nitrile group (N3···H9, 2.65; C1···H3, 2.89 Å). Phenyl and thiophene rings compactly stack on each other, correspondingly, with an interplane distance of approximately 3.7 Å. In the Y form, the largest $\mathbf{G}_\alpha$ is on the nitrile group; the nitro and amino groups also have large values. Three close contacts exist between molecules, including an intermolecular hydrogen bond, N3···H1 (2.42 Å). The other two are with the nitro group, O1···H9 (2.58 Å) and O2···C2 (3.12 Å). Stacking of phenyl rings is at an interplane distance of 3.8 Å. In the YN form, the largest $\mathbf{G}_\alpha$ is on N2; the nitrile, the N1 of the amino group, and C6–C8 of the phenyl ring also have significant values. Among the six close contacts, three originate from the nitro group, including an intermolecular hydrogen bond, O1···H1 (2.55 Å), O1···O1 (2.90 Å), and a unique N2···S1 contact (3.33 Å). Three close contacts, C5···H3 (2.90 Å), C7···C4 (3.32 Å), and C7···C7 (3.24 Å), appear to stabilize the stacking of the phenyl rings. Finally, in the YT04 form, $\mathbf{G}_\alpha$ values are generally smaller than those in other crystal forms. More interestingly, atoms of the nitro group have insignificant values. The largest value is found on N1; N3 also has a large value and forms one of two close contacts in the crystal of an intermolecular hydrogen bond (N3···H1, 2.55 Å). Two phenyl rings are stacked at an interplane distance of 3.5 Å and then sandwiched by two thiophene molecules, which leads to another close contact, C5···C12 (3.31 Å).

It is evident that the various functional groups of the ROY molecule exhibit distinct crystallization forces and the same functional group may have different values depending on the crystal structure. Large values are normally associated with close contacts, which include hydrogen bonds, formed between neighboring molecules. The nitro group, except in the YT04 form, has a large $\mathbf{G}_\alpha$ and is involved in 10 of the 20 close contacts that are identified in the seven crystal structures. The nitrile group, which displays a large $\mathbf{G}_\alpha$, contributes to five close contacts. The remaining five close contacts are mostly due to the stacking of phenyl and thiophene rings, which also leads to intermolecular contacts at interplane distances of 3.5–4 Å. The carbon atoms of the phenyl ring, particularly C6 and C8, generally show large $\mathbf{G}_\alpha$ values.

Lattice energies: The connection between large crystallization forces and close contacts suggests that the crystallization force is capable of describing the locality of intermolecular interactions that develop from the self-assembly process of crystallization. More likely, the concept may be able to determine the binding strength of a crystal system. To further explore the importance of the concept, the lattice energies of ROY polymorphs were calculated by the empirically augmented DFT method[4] and are listed in Table 5. Since three damping functions were used for calculating the van der Waals energy, three different values of lattice energy were obtained for each polymorph. Despite the significant difference among the three values, the ranking orders of the polymorphs from their thermodynamic lattice energies, $E_{lattice}$, and their relative differences are not affected by the selection of the damping function. The thermodynamic stability at zero Kelvin can be sorted as ORP > ON > Y > R > OP > YN > YT04, with ORP the most stable and the YT04 the least stable. There is a large difference in $E_{lattice}$ (ca. 20 kJ mol^{-1}) between the ORP and YT04 forms, but the difference among the six forms, excluding YT04, is smaller (ca. 13 kJ mol^{-1}). The $E_{lattice}$ values of the Y, R, and OP forms are extremely close. Figure 6 shows plots of the lattice energy calculated by using each of the three damping functions for the empirical component, versus the total crystallization force, G [Eq. (11)], of each polymorph. Linear correlations are indicated by the R^2 values of least-square linear regression between the two variables. $E_{crystal}$, not $E_{lattice}$, is used as the lattice energy in the regression because the energy term considers no conformational change from the gas to solid phase for the energy evaluation, in a similar way as the crystallization force is calculated. So it may be regarded as a kinetic energy term as compared with $E_{lattice}$, which considers the conformational change and is thereby a thermodynamic term. Good correlations can be seen in Figure 6, with that between the lattice energy evaluated by the damping function #1 and crystallization force beings especially strong. Because of the close connection between lattice energy and total crystallization force, it is compelling to believe that the crystallization force can characterize the intermolecular interaction in a crystal form that is generated by the crystallization process. And the overall scale of the total crystallization force should underline the stability of a crystal structure. For the case of ROY, the small energy differences among the polymorphs likely arise from the close con-

Table 5. Lattice energies (in kJ mol^{-1}) of ROY polymorphs. The three damping functions were used to compute the empirical components of the van der Waals energy in the crystals.[4] The difference between $E_{crystal}$ and $E_{lattice}$ is the energy evaluation of a single molecule in the gas phase. For $E_{crystal}$, the same conformation as in a crystal structure was used, whereas the global minimum of a single molecule was used for $E_{lattice}$.

	$E_{crystal}$			$E_{lattice}$		
	Damping function #1	Damping function #2	Damping function #3	Damping function #1	Damping function #2	Damping function #3
ORP	−117.676	−110.836	−102.056	−114.803	−107.963	−99.183
ON	−119.281	−110.771	−99.001	−111.164	−102.654	−90.884
Y	−122.857	−114.397	−104.667	−107.121	−98.661	−88.931
R	−119.465	−112.445	−103.115	−104.435	−97.415	−88.085
OP	−112.783	−106.083	−96.533	−103.469	−96.769	−87.219
YN	−115.611	−110.911	−102.271	−99.265	−94.565	−85.925
YT04	−114.334	−104.704	−93.224	−97.584	−87.954	−76.474

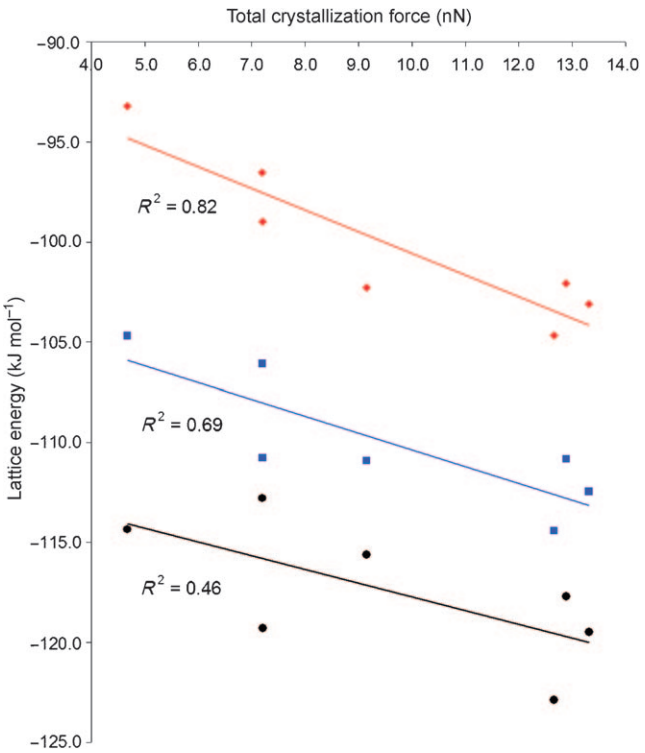

Figure 6. Lattice energies versus the total crystallization forces along with the trend lines plotted for all polymorphs. The R^2 values of the linear fitting are marked next to the trend lines. Note $E_{crystal}$ (Table 5) is used as the lattice energy. Data were obtained with damping function #1 (◆), #2 (■), or #3 (●).

tacts that are generally in agreement with large crystallization forces. As the damping function becomes weaker in reducing the van der Waals component at short interatomic distance (from #1 to #2 to #3), the correlation indicated by the R^2 value becomes poorer (from 0.82 to 0.69 to 0.46). This is understandable because the damped van der Waals energy is of long range and should have a minor or trivial footprint when the interatomic distance is small. Thus, the correlation can be useful for identifying a proper damping function (by yielding a high R^2 value). Conversely, a better model for calculating lattice energy may yield a closer correlation between the lattice energy and total crystallization force of a polymorphic system. What is more interesting here is the strong connection between the electronic concept, crystallization force, and the lattice energy that is evaluated by an empirically augmented DFT method. The relationship supports the validity of the DFT concept in describing intermolecular interactions, particularly those determining various molecular-packing motifs of a polymorphic system.

Thus, from the analyses of the molecular conformations and crystallization forces of ROY polymorphs, the polymorphism of ROY is believed to be a collective result of several functional groups—including the nitro, nitrile, amino, and aromatic rings—that participate in the stronger intermolecular interactions rather than long-range van der Waals forces, thereby forming close contacts including intermolecular hydrogen bonds. The nature of the close contact lies in the sharing of electrons, which is revealed and likely quantified by the crystallization force that characterizes the local change in electronic structure of a molecular system induced by the self-assembly process of crystallization.

Because of the symmetry between molecules in a crystal system, the "net", total crystallization force in a unit cell should be zero in spite of the crystallization forces on a molecule (e.g., illustrated in Figure 5) being unsymmetrical with respect to the shape of the molecule. However, in this report, the directionality of a crystallization force was not examined, but it is believed to play an important role in local packing motifs of molecules. In addition, to improve the numerical accuracy of the crystallization force values, different population schemes need to be tested for obtaining higher quality atomic charges in the gas and solid phases. Clearly, more studies are warranted to examine this DFT-based concept, crystallization force, for its validity and applicability.

Conclusion

Crystallization force, a concept developed from the Fukui function, aims to characterize and quantify the locality of intermolecular interactions in an organic crystal structure. It is regarded as a normalized nuclear Fukui function, with the normalization chosen to reflect the changes in electronic structure associated with the self-assembly process of crystallization. Calculated crystallization force values of seven polymorphs of ROY support the intended claim that large crystallization forces are generally associated with strong intermolecular interactions including close contacts and hydrogen bonds. The absolute values of the total crystallization force show significant correlation with the lattice energies of the polymorphs, further supporting the concept of the crystallization force in quantifying the binding of molecules in a crystal.

Acknowledgements

The research was supported by the NSF (DMR-0449633). C.A.M. acknowledges her gratitude to the University of Kentucky Center for Computational Sciences for her fellowship.

[1] a) S. R. Byrn, R. R. Pfeiffer, J. G. Stowell, *Solid-State Chemistry of Drugs*, SSCI, Inc., West Lafayette, Indiana, **1999**; b) J. Bernstein, *Polymorphism in Molecular Crystals*, Clarendon Press, Oxford, **2002**.

[2] a) J. P. M. Lommerse, W. D. S. Motherwell, H. L. Ammon, J. D. Dunitz, A. Gavezzotti, D. W. M. Hofmann, F. J. J. Leusen, W. T. M. Mooij, S. L. Price, B. Schweizer, M. U. Schmidt, B. P. van Eijck, P. Verwer, D. E. Williams, *Acta Crystallogr. Sect. A* **2000**, *56*, 697–714; b) W. D. S. Motherwell, H. L. Ammon, J. D. Dunitz, A. Dzyabchenko, P. Erk, A. Gavezzotti, D. W. M. Hofmann, F. J. J. Leusen, J. P. M. Lommerse, W. T. M. Mooij, S. L. Price, H. Scheraga, B. Schweizer, M. U. Schmidt, B. P. van Eijck, P. Verwer, D. E. Williams, *Acta Crystallogr. Sect. A* **2002**, *58*, 647–661; c) G. M. Day, W. D. S. Motherwell, H. L. Ammon, S. X. M. Boerrigter, V. R. G. Della, E. Venuti,

A. Dzyabchenko, J. D. Dunitz, B. Schweizer, B. P. van Eijck, P. Erk, J. C. Facelli, V. E. Bazterra, M. B. Ferraro, D. W. M. Hofmann, F. J. J. Leusen, C. Liang, C. C. Pantelides, P. G. Karamertzanis, S. L. Price, T. C. Lewis, H. Nowell, A. Torrisi, H. A. Scheraga, Y. A. Arnautova, M. U. Schmidt, P. Verwer, *Acta Crystallogr. Sect. A* **2005**, *61*, 511–527.

[3] T. Beyer, T. Lewis, S. L. Price, *CrystEngComm* **2001**, *3*, 213–216.

[4] a) S. Feng, T. Li, *J. Chem. Theory Comput.* **2006**, *2*, 149–156; b) T. Li, S. Feng, *Pharm. Res.* **2006**, *23*, 2326–2332.

[5] M. A. Neumann, F. J. J. Leusen, J. Kendrick, *Angew. Chem.* **2008**, *120*, 2461–2464; *Angew. Chem. Int. Ed.* **2008**, *47*, 2427–2430.

[6] a) M. C. Etter, *Acc. Chem. Res.* **1990**, *23*, 120–126; b) J. Bernstein, R. E. Davis, L. Shimoni, N. L. Chang, *Angew. Chem.* **1995**, *107*, 1689–1708; *Angew. Chem. Int. Ed. Engl.* **1995**, *34*, 1555–1573; c) G. R. Desiraju, *Acc. Chem. Res.* **2002**, *35*, 565–573; d) T. Steiner, *Angew. Chem.* **2002**, *114*, 50–80; *Angew. Chem. Int. Ed.* **2002**, *41*, 48–76.

[7] P. Metrangolo, G. Resnati, T. Pilati, S. Biella, *Structure & Bonding, Vol. 126*, Springer, Berlin, **2008**, pp. 105–136.

[8] a) F. J. M. Hoeben, P. Jonkheijm, E. W. Meijer, A. Schenning, *Chem. Rev.* **2005**, *105*, 1491–1546; b) E. A. Meyer, R. K. Castellano, F. Diederich, *Angew. Chem.* **2003**, *115*, 1244–1287; *Angew. Chem. Int. Ed.* **2003**, *42*, 1210–1250.

[9] a) C. B. Aakeroy, *Acta Crystallogr. Sect. A* **1997**, *53*, 569–586; b) J. D. Dunitz, A. Gavezzotti, *Angew. Chem.* **2005**, *117*, 1796–1819; *Angew. Chem. Int. Ed.* **2005**, *44*, 1766–1787.

[10] P. Vishweshwar, J. A. McMahon, J. A. Bis, M. J. Zaworotko, *J. Pharm. Sci.* **2006**, *95*, 499–516.

[11] a) C. Aubrey-Medendorp, M. J. Swadley, T. Li, *Pharm. Res.* **2008**, *25*, 953–959; b) T. Li, *J. Pharm. Sci.* **2007**, *96*, 755–760.

[12] L. Yu, G. A. Stephenson, C. A. Mitchell, C. A. Bunnell, S. V. Snorek, J. J. Bowyer, T. B. Borchardt, J. G. Stowell, S. R. Byrn, *J. Am. Chem. Soc.* **2000**, *122*, 585–591.

[13] S. Chen, I. A. Guzei, L. Yu, *J. Am. Chem. Soc.* **2005**, *127*, 9881–9885.

[14] a) P. Hohenberg, W. Kohn, *Phys. Rev. B* **1964**, *136*, B864–B871; b) W. Kohn, A. D. Becke, R. G. Parr, *J. Phys. Chem.* **1996**, *100*, 12974–12980; c) R. G. Parr, W. T. Yang, *Annu. Rev. Phys. Chem.* **1995**, *46*, 701–728.

[15] a) H. Nakatsuji, *J. Am. Chem. Soc.* **1974**, *96*, 24–30; b) H. Nakatsuji, *J. Am. Chem. Soc.* **1974**, *96*, 30–37.

[16] a) R. G. Parr, W. T. Yang, *J. Am. Chem. Soc.* **1984**, *106*, 4049–4050; b) W. Yang, R. G. Parr, R. Pucci, *J. Chem. Phys.* **1984**, *81*, 2862–2863; c) P. Geerlings, F. De Proft, W. Langenaeker, *Chem. Rev.* **2003**, *103*, 1793–1873.

[17] P. W. Ayers, M. Levy, *Theor. Chem. Acc.* **2000**, *103*, 353–360.

[18] a) M. Berkowitz, R. G. Parr, *J. Chem. Phys.* **1988**, *88*, 2554–2557; b) Y. Simon-Manso, P. Fuentealba, *J. Phys. Chem. A* **1998**, *102*, 2029–2032; c) P. W. Ayers, *Faraday Discuss.* **2007**, *135*, 161–190.

[19] A. Vela, J. L. Gázquez, *J. Am. Chem. Soc.* **1990**, *112*, 1490–1492.

[20] a) R. G. Pearson, *J. Am. Chem. Soc.* **1963**, *85*, 3533–3539; b) R. G. Pearson, *Science* **1966**, *151*, 172–177; c) R. G. Parr, R. G. Pearson, *J. Am. Chem. Soc.* **1983**, *105*, 7512–7516; d) P. K. Chattaraj, H. Lee, R. G. Parr, *J. Am. Chem. Soc.* **1991**, *113*, 1855–1856.

[21] P. W. Ayers, R. G. Parr, R. G. Pearson, *J. Chem. Phys.* **2006**, *124*, 194107.

[22] M. Berkowitz, *J. Am. Chem. Soc.* **1987**, *109*, 4823–4825.

[23] J. S. M. Anderson, J. Melin, P. W. Ayers, *J. Chem. Theory Comput.* **2007**, *3*, 358–374.

[24] a) G. Klopman, *J. Am. Chem. Soc.* **1968**, *90*, 223–234; b) R. G. Parr, W. Yang, *Density-Functional Theory of Atoms and Molecules*, Oxford University Press, New York, NY, **1989**.

[25] W. T. Yang, R. G. Parr, *Proc. Natl. Acad. Sci. USA* **1985**, *82*, 6723–6726.

[26] K. Morokuma, *Acc. Chem. Res.* **1977**, *10*, 294–300.

[27] S. Liu, *J. Chem. Phys.* **2007**, *126*, 244103–244105.

[28] a) J. P. Perdew, R. G. Parr, M. Levy, J. L. Balduz, *Phys. Rev. Lett.* **1982**, *49*, 1691–1694; b) W. T. Yang, Y. K. Zhang, P. W. Ayers, *Phys. Rev. Lett.* **2000**, *84*, 5172–5175.

[29] a) M. H. Cohen, M. V. Ganduglia-Pirovano, J. Kudrnovsky, *J. Chem. Phys.* **1994**, *101*, 8988–8997; b) F. De Proft, S. Liu, P. Geerlings, *J. Chem. Phys.* **1998**, *108*, 7549–7554; c) R. Balawender, F. De Proft, P. Geerlings, *J. Chem. Phys*, **2001**, *114*, 4441–4449.

[30] a) H. Hellmann, *Einführung in die Quantenchemie*, Deuticke, Leipzig, **1937**; b) R. P. Feynman, *Phys. Rev.* **1939**, *56*, 340–343.

[31] a) W. Yang, W. J. Mortier, *J. Am. Chem. Soc.* **1986**, *108*, 5708–5711; b) P. Fuentealba, P. Perez, R. Contreras, *J. Chem. Phys.* **2000**, *113*, 2544–2551; c) P. Bultinck, S. Fias, C. Van Alsenoy, P. W. Ayers, R. Carbo-Dorca, *J. Chem. Phys.* **2007**, *127*.

[32] P. W. Ayers, R. C. Morrison, R. K. Roy, *J. Chem. Phys.* **2002**, *116*, 8731–8744.

[33] a) P. Bultinck, R. Carbo-Dorca, *J. Math. Chem.* **2003**, *34*, 67–74; b) P. Bultinck, R. Carbo-Dorca, W. Langenaeker, *J. Chem. Phys.* **2003**, *118*, 4349–4356; c) J. Melin, P. W. Ayers, J. V. Ortiz, *J. Phys. Chem. A* **2007**, *111*, 10017–10019; d) P. W. Ayers, *Phys. Chem. Chem. Phys.* **2006**, *8*, 3387–3390.

[34] a) R. K. Roy, S. Pal, K. Hirao, *J. Chem. Phys.* **1999**, *110*, 8236–8245; b) R. K. Roy, K. Hirao, S. Pal, *J. Chem. Phys.* **2000**, *113*, 1372–1379.

[35] a) A. D. Becke, *Phys. Rev. A* **1988**, *38*, 3098–3100; b) C. T. Lee, W. T. Yang, R. G. Parr, *Phys. Rev. B* **1988**, *37*, 785–789.

[36] R. Dovesi, R. Orlando, B. Civalleri, C. Roetti, V. R. Saunders, C. M. Zicovich-Wilson, *Z. Kristallogr.* **2005**, *220*, 571–573.

[37] D. Thompson, J. Braun, R. Ford, *OpenDX: Paths to Visualization*, VIS, Inc., Missoula, MT, **2000**.

[38] Gaussian 03, Revision B.05, M. J. Frisch, G. W. Trucks, H. B. Schlegel, G. E. Scuseria, M. A. Robb, J. R. Cheeseman, J. A. Montgomery, Jr., T. Vreven, K. N. Kudin, J. C. Burant, J. M. Millam, S. S. Iyengar, J. Tomasi, V. Barone, B. Mennucci, M. Cossi, G. Scalmani, N. Rega, G. A. Petersson, H. Nakatsuji, M. Hada, M. Ehara, K. Toyota, R. Fukuda, J. Hasegawa, M. Ishida, T. Nakajima, Y. Honda, O. Kitao, H. Nakai, M. Klene, X. Li, J. E. Knox, H. P. Hratchian, J. B. Cross, V. Bakken, C. Adamo, J. Jaramillo, R. Gomperts, R. E. Stratmann, O. Yazyev, A. J. Austin, R. Cammi, C. Pomelli, J. W. Ochterski, P. Y. Ayala, K. Morokuma, G. A. Voth, P. Salvador, J. J. Dannenberg, V. G. Zakrzewski, S. Dapprich, A. D. Daniels, M. C. Strain, O. Farkas, D. K. Malick, A. D. Rabuck, K. Raghavachari, J. B. Foresman, J. V. Ortiz, Q. Cui, A. G. Baboul, S. Clifford, J. Cioslowski, B. B. Stefanov, G. Liu, A. Liashenko, P. Piskorz, I. Komaromi, R. L. Martin, D. J. Fox, T. Keith, M. A. Al-Laham, C. Y. Peng, A. Nanayakkara, M. Challacombe, P. M. W. Gill, B. Johnson, W. Chen, M. W. Wong, C. Gonzalez, J. A. Pople, Gaussian, Inc., Wallingford CT, **2004**.

[39] Q. Wu, W. T. Yang, *J. Chem. Phys.* **2002**, *116*, 515–524.

[40] T. A. Halgren, *J. Am. Chem. Soc.* **1992**, *114*, 7827–7843.

[41] A. Bondi, *J. Phys. Chem.* **1964**, *68*, 441–451.

Received: May 31, 2008
Revised: August 29, 2008
Published online: November 25, 2008

